JOURNAL OF BACTERIOLOGY, July 1980, p. 481-491
0021-9193/80/07-0481/11$02.00/00

Vol. 143, No. 1

Distribution of Calcium and Other Elements in Cryosectioned *Bacillus cereus* T Spores, Determined by High-Resolution Scanning Electron Probe X-Ray Microanalysis

MURRAY STEWART,[1,2]* ANDREW P. SOMLYO,[2] AVRIL V. SOMLYO,[2] HENRY SHUMAN,[2] J. A. LINDSAY,[3] AND W. G. MURRELL[3]

CSIRO Division of Computing Research, P.O. Box 1800, Canberra City, ACT 2601, Australia,[1] Pennsylvania Muscle Institute, University of Pennsylvania, Philadelphia, Pennsylvania 19104,[2] and CSIRO Division of Food Research, North Ryde, NSW 2113, Australia[3]

The distribution of a number of key elements in *Bacillus cereus* T spores was determined by high-resolution scanning electron probe X-ray microanalysis. To circumvent the redistribution of soluble or weakly bound elements, freeze-dried cryosections of spores, which had been rapidly frozen in 50% aqueous polyvinyl pyrrolidone, were employed. The sections were examined by using a modified Philips EM400 electron microscope fitted with a field emission gun, scanning transmission electron microscopy attachment, and a computer-linked energy-dispersive X-ray microanalysis system. X-ray maps for selected elements and the corresponding electron image were produced simultaneously by scanning the cryosections with a fine electron beam in a raster pattern, using the scanning transmission electron microscopy attachment. The results indicated that almost all of the calcium, magnesium, and manganese, together with most of the phosphorus, was located in the core region. An unexpectedly high concentration of silicon was found in the cortex/coat layer. Granules containing high concentrations of calcium, manganese, and phosphorus were demonstrated in spores containing reduced levels of dipicolinic acid. Spot mode analyses, in which a stationary beam was located over the region of interest in the spore cryosection, confirmed the results obtained with the scanning mode and also provided a more accurate quantitation of the elemental concentrations on a dry weight basis.

Bacterial spores show remarkable physiological properties, in particular a resistance to heat, radiation, enzymes, disinfectants, and other normally deleterious agents (30). Furthermore, they have no detectable metabolism when dormant and yet are able to germinate in a matter of minutes and ultimately form vegetative cells. Spores of all species have the same general morphology, consisting of an inner core (protoplast) surrounded by, in turn, a germ cell wall, cortex, coats, and, in some species, an exosporium. They may, however, differ dramatically in their resistance and stability. Spores also have a distinctive composition which is quite unlike that of vegetative cells, particularly with respect to low concentrations of sodium and chlorine and greatly elevated concentrations of 3-phosphoglyceric acid, dipicolinic acid, calcium, and manganese (19, 30). The high concentration of divalent cations is a consequence of their rapid uptake in stage IV of sporulation (33) and may ultimately comprise up to 3% of the dry weight of the spore (22). These cations are rapidly released during germination and are associated with spore dormancy and resistance. The ratio of the concentration of calcium ions to magnesium ions and the dipicolinic acid concentration appear to be major factors associated with heat resistance (22). It has been suggested that cations are critically involved in four postulated basic mechanisms of spore heat resistance, namely, the contractile cortex theory (16, 21), the protective chelate cement theory (10), the expanded cortex theory (9), and the syneresed protoplast model (3, 17). Calcium is also believed to have at least two distinct physiologically active sites in spores (18), as indicated by its roles in germination, heat resistance, and heat adaptation. The levels of manganese also appear to influence radiation resistance (2). The implication of these ions in any model of spore resistance or dormancy is, of course, critically dependent on their precise locations within spores.

Several attempts have been made to determine the distribution of inorganic ions within bacterial spores. Whole spores have been examined by light (13) and electron (28) microscopy after microincineration. The ash remaining (presumed to represent mainly inorganic material) tends to be concentrated towards the center

of the spore, indicating that a substantial proportion of these ions may be located in the core. However, this interpretation is complicated by the difficulty in compensating for changes in thickness (the thickest part of the spore is at the center, and so one would expect there to be more material there anyway) and possible contraction of the ash or redistribution of elements during incineration. Attempts have also been made to examine sectioned spores, but these were limited by possible diffusion of the elements during sample preparation and by an inability to preserve the spore cortex (28).

Scherrer and Gerhardt (23) employed electron probe X-ray microanalysis to examine both whole spores and conventionally embedded and sectioned material. This technique enables elemental determinations to be made on small areas of specimens by analyzing the X-rays produced when the area is irradiated by a fine electron beam (see reference 11, for a review of the principles involved). The resolution obtained on whole spores was very low (500 to 1,000 nm, which is the same order as the dimensions of the spore), which, when combined with the pronounced thickness changes across the specimen and the fact that there was no method by which the core could be located in the spore (save for its central location), made interpretation difficult. The distribution of calcium essentially paralleled that of carbon. Similar results for whole spores were obtained by Ando (1). Scherrer and Gerhardt (23) also examined sections obtained from spores embedded in epoxy resin and stained with heavy-metal salts. However, the ultrastructure of the spore could not be observed directly during X-ray analyses, and it was necessary to relate the microanalysis results to micrographs subsequently recorded in a transmission electron microscope. It was impossible to ensure that calcium was not redistributed during embedding or that some calcium might not have been exchanged by uranium. However, it was suggested that about 80% of the spore calcium could be located in the protoplast. X-ray photoelectron microscopy (29) has indicated a peripheral location for some calcium.

Since Scherrer and Gerhardt's study, there have been a number of improvements in both instrumentation and sample preparation. For example, resolutions of at least 20 nm have been obtained on biological specimens by employing scanning transmission electron microscopy (STEM) in conjunction with a field emission gun (27), whereas rapid freezing combined with cryosectioning has allowed preparation of biological specimens in which the redistribution of soluble or weakly bound ions is circumvented. The success with which these techniques have recently been applied to study calcium distribution in muscle specimens (25, 26) prompted us to employ them to examine the distribution of a number of key elements in *Bacillus cereus* T spores. This has enabled us to refine and extend the earlier studies and to determine directly the elemental distribution of calcium, manganese, phosphorus, magnesium, silicon, and sulfur at high resolution and relate it to the ultrastructure of the spore.

MATERIALS AND METHODS

Spores. Spores of *B. cereus* T wild type and of a *B. cereus* dipicolinic acid-minus mutant (strain HW1) were grown and prepared as described previously (21). They were washed with three changes of glass-distilled water, followed by 0.02 M HCl for 10 min (to remove inorganic precipitates derived from the nutrient medium and also adhering fragments of the parent cell cytoplasm), and then with three more washes in glass-distilled water before being freeze-dried. All of the manipulations were carried out at 1°C. Silicone antifoam agents were not employed. Determination of the stage of forespore development within a sporulating culture and subsequent analysis of the cells by electron microscopy were performed as described previously (21).

Sample preparation. Before examination, the dried spores were rehydrated in distilled water for several hours and then examined by phase-contrast light microscopy to check that germination had not been initiated. They were then pelleted in a bench centrifuge, mixed with an equal volume of 50% (wt/vol) aqueous polyvinyl pyrrolidone (PVP, pharmaceutical grade; average molecular weight, 40,000; Sigma Chemical Co., St. Louis, Mo.; purified as described in reference 4) and frozen rapidly in supercooled Freon 22 (E. I. du Pont de Nemours & Co., Inc., Wilmington, Del.) at -164 ± 2°C as described in detail previously (25, 26). Some spores were also frozen in distilled water only but were much more difficult to cut and tended to break up before they could be collected on grids. Cryosections about 100 to 200 nm thick were cut and freeze-dried as described previously (25). Some pellets frozen in 50% PVP were also embedded in epoxy resin by the freeze-substitution method described in detail elsewhere (5). Mounts of whole spores were prepared by dusting them directly onto carbon-coated grids.

Electron probe X-ray microanalysis. Specimens were examined in a Philips EM400 transmission electron microscope fitted with a goniometer stage, field emission gun, STEM attachment, and a 30-mm^2 (20° specimen-to-detector angle, 0.067 steradians solid angle, 160 eV resolution) Kevex Si(Li) energy-dispersive X-ray detector (Kevex Corp., Foster City, Calif.) and a Kevex model 7000 multichannel analyzer interfaced to a PDP 11/34 computer system (Digital Equipment Corp., Maynard, Mass.). The equipment configuration is illustrated in Fig. 1, and its operating characteristics have been described in detail elsewhere (24–27). Information from the electron and X-ray detector systems was collected on-line and stored on a magnetic disk until required for processing. The microscope was operated at an acceleratering voltage of 80 kV and a

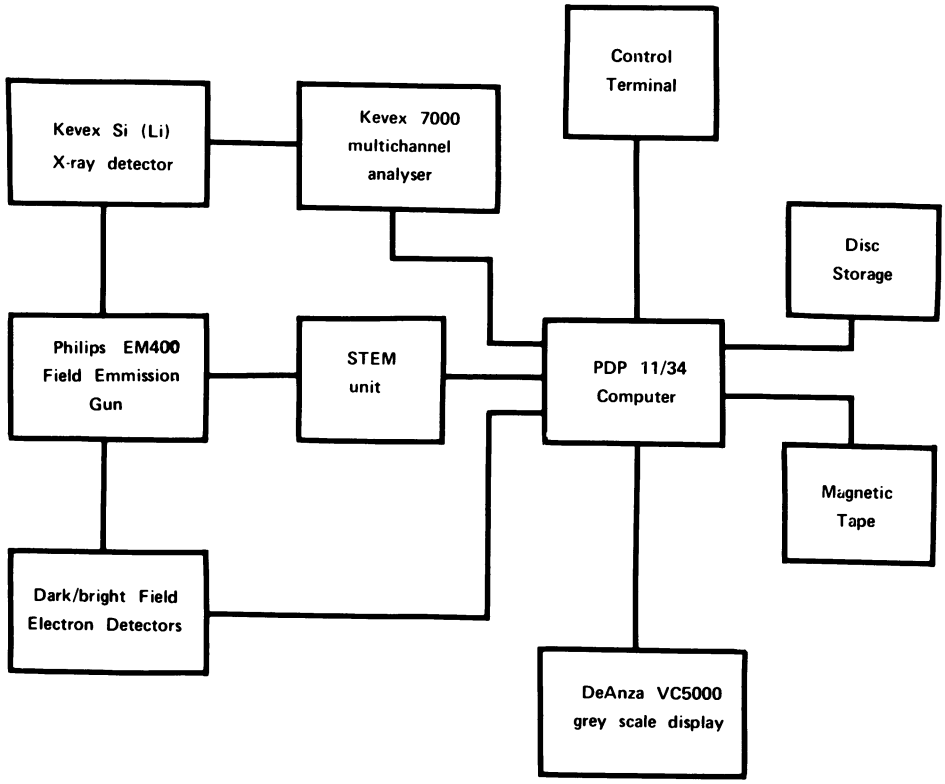

FIG. 1. *Equipment configuration employed for high-resolution electron probe X-ray microanalysis.*

probe current of approximately 10 nA. Probe sizes as small as 1.5 nm could be obtained.

The X-ray spectrum obtained in a transmission electron optical column from a thin section of biological material includes the characteristic peaks due to elements with atomic numbers greater than 10 present in the specimen and the associated continuum largely arising from the organic matrix (see Fig. 2). The spectrum also contains instrumental peaks (the largest one being due to copper at 8.047 keV) from the specimen grid and holder, with an associated extraneous continuum, and low-energy noise probably due to electrons reaching the detector. These extraneous signals can be determined and subtracted from the spectrum (24).

The specimens were analyzed in two ways. In the first, maps of the distribution of particular elements were produced by scanning large areas of the specimen with a fine beam. In these maps, quantitation was limited because of Poisson noise associated with the short time interval (generally about 2 ms) for which the beam resided at each point making up the final image. Consequently, these maps should only be taken to indicate the distribution of an element and its regularity. Furthermore, in this mode, the signal will also contain continuum contributions, and some of these could reflect artifacts associated with mass differences across the specimen. In the present instance, this effect was small, since continuum maps, recorded simultaneously with other X-ray maps, contained relatively few counts and did not show any of the features seen in the others.

The second type of procedure involved spot mode analysis and enabled accurate quantitation of selected areas of the image, which could be as small as 10 to 20 nm but which were usually larger. In this mode, the beam was allowed to reside on the area of interest until accurate counting statistics were obtained. In addition, corrections were made for continuum contributions, and concentrations could be expressed on a dry mass basis (see below).

Maps for particular elements were generated by using the STEM attachment to perform a raster scan and, at each picture point, recording the number of X-ray counts occurring in a narrow window centered on the energy characteristic for the element. Generally, images were built up from 512 lines, each containing 512 picture elements (i.e., a total of 262,144 picture elements), and involved a counting time of 1 s per line or about 2 ms per picture element. Up to four maps and one image could be collected simultaneously. Figure 2 illustrates the windows used for the particular elements and for the continuum. Gray-scale images were generated on a video screen by using a DeAnza VC5000 image display system (De Anza Corp, San Jose, Calif.) which enables 16 bits of information to be stored for an image of up to 512 × 512 picture elements. The images shown in Fig. 4 and 5 are photographs taken directly from the screen of this device.

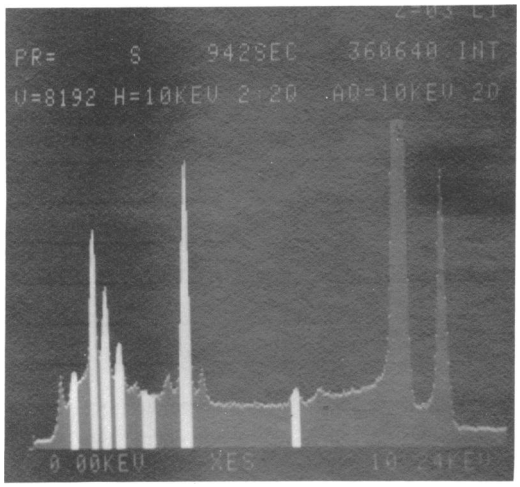

FIG. 2. *Typical X-ray spectrum from a raster scan of a wild-type spore, illustrating the windows employed for each element (lighter). From left to right these are magnesium, silicon, phosphorus, sulfur, continuum, calcium, and manganese. Windows were 230 eV wide and centered on the energy characteristic for each element. The two large peaks at the extreme right represent copper from the support grid. The vertical axis is number of counts (full scale is 8,192), and the horizontal axis is energy (0 to 10.24 keV). The total accumulation time was 942 s, and the total calcium counts accumulated was 360,640.*

For the spot mode analyses, cryosections were examined in a cold stage at approximately −165°C as described previously (25, 26), with the instrument operated in the conventional transmission electron microscopy mode. In the case of cores, the beam diameter was adjusted so that it occupied most of the core region. For the cortex/coat layer, the spot was elongated with the condenser stigmator to enable a larger area to be measured. In this instance, beams with an aspect ratio of between about 2:1 and 5:1 were employed, with the size adjusted so that the spot lay only in the area corresponding to the cortex/coat layer. Although the ultrastructure of the specimen was not visible when the beam was finally focused, the specimen morphology could be seen with the beam slightly expanded, and so the detailed positioning of the spot did not present any difficulty. The position was checked at approximately 20-s intervals to ensure that it had not drifted (counting was, of course, stopped during these periods). Generally, areas were counted for 100 s. Concentrations of particular elements were obtained by a least-squares analysis of the spectra, and the dry mass of the area examined was derived from the continuum region of the spectrum as described in detail previously (24). The measurement of elemental concentrations is based on the fact, pointed out by Hall (11), that for elements of atomic number greater than 10 in concentrations of less than 1 mol/kg (dry weight) in thin sections, the characteristic peak-to-continuum ratio is linearly related to the concentration-to-dry mass ratio. Thus, absolute concentrations can be obtained by comparing peak counts (after subtracting continuum background) to the standards and also to the counts obtained in a separate continuum window located where there will be few counts due to characteristic X-rays (we employed a continuum window between 1.34 and 1.64 keV, which gives best results in samples lacking aluminium). The values obtained by X-ray microanalysis were comparable to those obtained by atomic absorption analysis of bulk samples (Table 1).

Chemical analyses. Dipicolinic acid was analyzed by the method of Warth (31), in which the dipicolinic acid was extracted from the spores by heating in 20 volumes of 4 M potassium phosphate buffer (pH 1.8) at 100° C for 10 min. It was then assayed by liquid chromatography over Merck Lichrosorb RP8 (0.01-mm particle size; Merck, Darmstadt, Germany) and elution with 1.5% *t*-amyl alcohol in 0.2 M potassium phosphate buffer (pH 1.8 at 25°C). Absorbance was measured at 271 nm. Divalent cations were assayed by atomic absorption spectrometry in a Varian Techtron AA6 spectrometer after the spores were digested in 6 M redistilled HCl for 18 h at 50°C.

RESULTS

Spore morphology. Samples of spores frozen in distilled water were very difficult to cryosection and tended to crumble before they could be picked up on grids. Examination of the fragments which could be picked up indicated that only the cores were well preserved, the outer layers having become disrupted during sectioning.

Spores frozen in 50% aqueous PVP proved much easier to cryosection and did not break up to the same extent on the knife. Cryosections suitable for electron-probe X-ray microanalysis could be obtained from this material without great difficulty.

Because cryosections are examined in an electron microscope without heavy metal stains, it is not easy to assess the degree to which the spore ultrastructure is preserved. Therefore, to ensure that the spore morphology had not been radically altered by freezing in 50% PVP, some sections prepared by freeze-substitution were also examined. Essentially, this involves replacing the frozen water in the specimen with acetone at a temperature sufficiently low that the water does not melt (below −80°C). The material is then embedded in epoxy resin by conventional procedures. Sections can then be stained and examined in the same way as for conventionally prepared material.

The stained material prepared by freeze-substitution was essentially the same as spores prepared by conventional procedures, indicating that the spore morphology was not greatly changed by the freezing step (Fig. 3). Exosporium, coats, cortex layers, and core were all clearly visible, and there was, for example, no obvious shrinkage of the cortex as a result of its

TABLE 1. *Comparison between results obtained by X-ray microanalysis of whole spores and determinations employing atomic absorption analysis of bulk samples of mutant HW1*

Method	No. of observations	Concn (mmol/kg, dry wt)			
		Ca	Mg	Mn	K
Atomic absorption	3	101 ± 2[a]	30 ± 1	5.6 ± 0.5	8.4 ± 0.5
X-ray microanalysis	10	108 ± 9	49 ± 9	8 ± 4	17 ± 6

[a] Mean ± standard error of the mean.

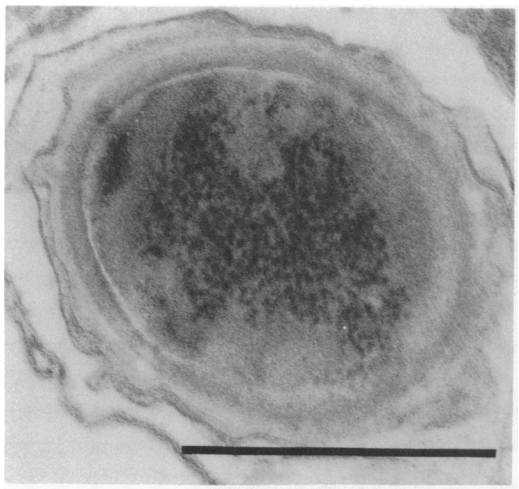

FIG. 3. *Transmission electron micrograph of a B. cereus T spore frozen in 50% aqueous PVP, embedded in epoxy resin by the freeze-substitution method (5), and then stained. The spore ultrastructure is well preserved, and the exosporium, coat, cortex layers, and core are all clear. Bar indicates 500 nm.*

contact with PVP. This observation is in accord with extensive studies made on a range of biological specimens (3), which indicated that PVP produced minimal structural damage. Furthermore, atomic absorption analysis of bulk spore samples treated with aqueous 50% PVP under these conditions indicated that there was no significant change in the spore calcium content.

STEM images of unstained spore cryosections were, of course, not highly contrasted. Because of this, it was difficult to photographically reproduce the image because the local contrast variations giving rise to the spore image were similar to the background variations over the image. (The problem is analogous to the difficulties often encountered in printing faint negatives on very-high-contrast paper, except that in this case one cannot "dodge.") However, one could still easily distinguish the core from the surrounding layers (there was a continuous dark boundary between the two) (Fig. 4a). Unfortunately, it was not possible to reproducibly distinguish between the cortex layers and the coat on these unstained sections. These features were well within the resolution capabilities of the instrument (27) and were clearly visible in stained epoxy resin sections prepared by freeze-substitution (Fig. 3). The difficulty in observing these structures in unstained cryosections was, therefore, not an artifact and was probably a result of both low contrast (associated with a small density difference between these components) and the curvature of these layers in the section. It also was not possible to distinguish the exosporium in the unstained cryosection, again probably because of its low intrinsic contrast and also possibly because it was too thin to be detected at the resolution to which we were working.

We therefore decided to restrict our study to determining the elemental distribution between the core and the cortex/coat layer considered as a whole, since the major physiological questions related to whether elements (particularly divalent cations) were located entirely in the core or not. Spot mode analyses of the cores of spores in cryosections prepared in either distilled water or 50% PVP were essentially the same, except that the absolute concentrations on a dry weight basis tended to be slightly higher in the spores frozen in water (although the difference was seldom more than one standard error). This may have been due to the PVP making some contribution to the dry mass of the spores, since the studies of Gerhardt and Black (6) indicate that some permeability of the spores to this substance might be expected. However, since the distribution of the elements, rather than their absolute concentration, was the object of our study, this was not considered to be a serious difficulty.

Wild-type spores. Typical results for wild-type *B. cereus* T spores are shown in Fig. 4 and Table 2. Figure 4b through h show X-ray maps corresponding to the STEM image in Fig. 4a. Because the continuum map (Fig. 4h) is featureless, one can be confident that real differences in elemental distribution (and not artifacts associated with mass distribution) are reflected in the other maps. There was an unexpectedly high concentration of silicon in the cortex/coat. Calcium, magnesium, and manganese were clearly confined to the core. The distribution of these divalent cations within the core, however, was essentially uniform, and there was no evidence for any clustering. Sulfur was distributed over

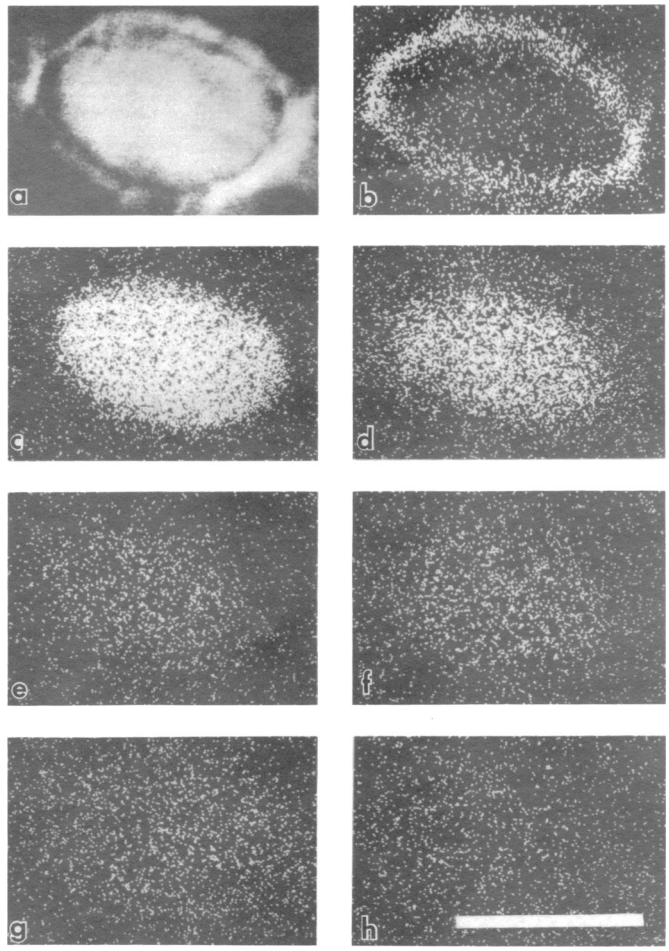

FIG. 4. *Images of a cryosectioned wild-type B. cereus T spore. (a) Unstained STEM image, using dark-field divided by bright-field mode. The core and outer cortex/coat layer are easily discerned. (b) Silicon map. (c) Calcium map. (d) Phosphorus map. (e) Magnesium map. (f) Manganese map. (g) Sulfur map. (h) Continuum map. Note that the divalent cations calcium, magnesium, and manganese are confined to the core region, along with most of the phosphorus. Silicon is strongly concentrated in the cortex/coat, whereas sulfur is distributed over the entire spore. The continuum map is featureless, indicating that the patterns observed in the other maps are not artifacts related to mass differences in the section. Bar indicates 500 nm.*

the entire structure. Most of the phosphorus was located in the core, with a smaller quantity located in the cortex/coat.

This distribution was confirmed, and more accurate measures of the concentrations of the various elements were obtained by examining cryosections with a stationary spot probe located over the region of interest (Table 2). One feature to emerge clearly from the spot mode analysis was a considerable variation in elemental composition between spores. Although this variation may be related partially to inhomogeneities in both the core and cortex layer, it seems likely that it also reflects a real difference between individual spores. This may be related to the change in composition of the sporulation medium with time, since sporulation is not a perfectly synchronous process.

Spores lacking dipicolinic acid. We also investigated *B. cereus* T spores in which the synthesis of dipicolinic acid was inhibited, either by employing a mutant (strain HW1, reference 21) that was unable to produce dipicolinic acid or by producing wild-type spores in a medium containing a low concentration of calcium (12). Essentially the same results were obtained with each type of spore, and so only those for the mutant will be described in detail here.

Both the core and the cortex/coat layer could be clearly distinguished (Fig. 5) and, in terms of

TABLE 2. *Composition data derived from spot mode analysis*

Object	Structure	No. of observations	Elemental concn[a] (mmol/kg, dry wt)						
			K	Mg	Ca	Mn	P	S	Si
Wild type in 50% PVP	Core	20	40 ± 5[b]	206 ± 11	693 ± 27	57 ± 3	472 ± 18	123 ± 4	45 ± 9
	Cortex/coat	20	7 ± 2	13 ± 3	12 ± 2	2 ± 1	53 ± 5	152 ± 15	162 ± 42
Wild type in water	Core	35	25 ± 4	220 ± 11	752 ± 40	60 ± 3	541 ± 28	84 ± 7	51 ± 11
PVP		4	1 ± 1	6 ± 5	−1 ± 4	3 ± 4	−3 ± 7	3 ± 5	26 ± 4
Mutant HW1 in 50% PVP	Whole core	20	0 ± 1	106 ± 6	164 ± 24	16 ± 1	678 ± 28	143 ± 5	30 ± 3
	Granule	7	1 ± 3	170 ± 11	867 ± 35	157 ± 17	1,429 ± 109	40 ± 8	41 ± 6
	Cortex/coat	20	2 ± 1	6 ± 3	16 ± 4	1 ± 1	107 ± 11	212 ± 16	90 ± 8

[a] Chlorine was determined in all samples but was only present in about the same concentration as the background and so was considered to be zero. The low concentrations of sodium present and the lower sensitivity of the apparatus for sodium (25) precluded its accurate measurement. Negative values are the result of statistical fluctuation in the least-squares method employed to determine concentrations (25, 26).

[b] Mean ± standard error of the mean.

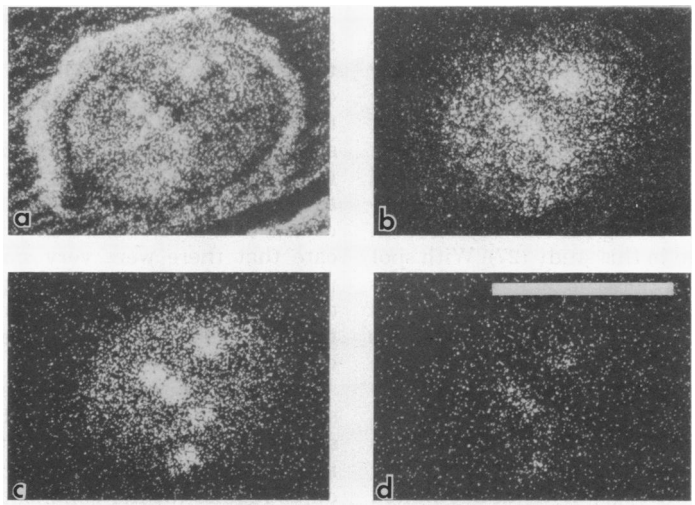

FIG. 5. *Images from B. cereus mutant (strain HW1) which lacks dipicolinic acid. (a) Unstained STEM image showing core, cortex, and core granules. (b) Phosphorus map. (c) Calcium map. (d) Manganese map. Note the correspondence between the images, indicating that the core granules contain highly elevated concentrations of manganese, calcium, and phosphorus. Bar indicates 500 nm.*

general size and shape, resembled those seen in the wild-type spores. However, the core region also appeared to contain a number of granules. Again, the divalent cations were essentially confined to the core region; however, in contrast to the maps of the wild-type spores, a distinct clustering was observed, which correlated with the granules visible in the STEM image (Fig. 5). Some clustering was also observed in the phosphorus map, but this was superimposed on a reasonably high background phosphorus signal. Spot analyses confirmed that these granules contained very high concentrations of phosphorus, manganese, and calcium. Their magnesium concentration was only about that of the rest of the core (Table 2), and their sulfur content was lower, suggesting that the granules may be composed of insoluble metal phosphates analogous to those found in mitochondrial granules (26). Similar granules were also observed in cryosections of the dipicolinic acid-depleted spores, produced by growing them in low-calcium medium. The spot mode analyses also indicated that the spores still contained a substantial concentration of calcium, even though chemical analysis indicated that they contained less than 0.01% of the dipicolinic acid found in the wild-type spores. This is in accord with earlier studies, which showed that, in the absence of exogenous dipicolinic acid, the mutant spores accumulated about 40% of the calcium content of the wild-type spores (21).

DISCUSSION

Reliability of determinations. Before proceeding to discuss the results obtained on the elemental distribution in *B. cereus* T spores, it is pertinent to consider the reliability of these determinations and also any factors in the sample preparative procedures which could have introduced artifacts.

By the use of freeze-dried cryosections, the possibility of elemental loss or redistribution was effectively circumvented. However, an important consideration when assessing the reliability of the data is the spatial resolution with which the elements have been localized, since earlier electron probe X-ray microanalysis studies (1, 23) were severely limited in this respect. Spatial resolution is influenced both by the size of the incident electron beam and by the degree to which it is spread while traversing the specimen. With thin cryosections, the spreading of the beam is very small (11) and does not greatly limit resolution. In the mapping studies, very small beam diameters were used (of the order of 2 to 5 nm), and so one would anticipate that resolutions of the order of 20 nm or better could be obtained. These have, in fact, been demonstrated on suitable biological test objects with the equipment used in this study (27). With spot mode analyses, the resolution similarly depends on the beam diameter and, if required, could easily be made better than 20 nm. However, this was not necessary in the present instance, since the areas being investigated were all considerably larger than this (for example, the cortex is about 100 nm wide). All that was necessary was to ensure that the beam was within the required boundaries. Thus, interpretation was not limited by spatial resolution, at least with respect to the bulk of each morphological unit.

It was not possible to be precise regarding the distribution at the cortex/core boundary for a number of reasons. In addition to the blurring due to a resolution limit of about 20 nm (which is appreciable when compared with the 5-nm resolution easily obtained with a transmission electron microscope), the curvature of the specimen meant that the actual boundary between these two areas was sometimes poorly defined. Occasionally, the two would seem to merge over short distances. However, this uncertainty only applies to the region of the cortex immediately adjacent to the core, and one could still be quite certain regarding the composition of the remainder (which represented 80 to 90% of the cortex region).

The signal-to-noise ratio of the information could also limit the confidence placed on the elemental distributions obtained. This is particularly so with respect to the X-ray maps, for which the counting times for each picture element were usually of the order of 2 ms. As a consequence, some of the maps were contaminated with Poisson noise. However, since the elemental concentrations did not vary rapidly with position and because the picture elements were placed much closer together than the theoretical value for an image of this resolution, this did not present major difficulties. The appearance of these maps improves greatly if one views them with one's eyes out of focus, whereby an approximate local averaging (caused by blurring of the image) tends to remove much of the Poisson noise.

These signal-to-noise problems were much less severe in the case of the spot mode analysis data, since one was able to count for much longer times. Consequently, concentrations here were known fairly accurately, except where the absolute concentrations were very low. The error due to background subtraction then became appreciable, and so the detection limit of the apparatus (with the counting parameters used in this study) was considered to be 5 to 10 mmol/kg (dry weight). Therefore, the values obtained for the concentrations of divalent cations in the cortex/coat layer should only be taken to indicate that there were very small quantities of these elements present (on the present evidence, one cannot really eliminate the null hypothesis that the concentration of these elements in the cortex/coat layer was zero).

Although the results obtained by freeze-substitution (Fig. 3) indicated that the spore ultrastructure was well preserved after rapid freezing in PVP, two aspects of the preparative procedures require further comment. The first is the possibility that the brief acid wash (used to remove surface inorganic precipitates derived from the nutrient medium and adhering vegetative matter) could also have removed some cations from the outermost layers of the spores. One cannot use bulk assays to confirm that no cations have been lost by this treatment, but a number of considerations make it seem unlikely that any were. The acid wash treatment was of short duration, at low temperature, and with dilute acid. Under these conditions, there is little evidence of any stripping of divalent cations (14; A. D. Warth, personal communication); more forcing conditions are generally required for this to occur (e.g., 2 M HCl at elevated temperatures). More important from the point of view of spore physiology is the fact that these spores are fully viable and heat resistant (22) after the treatment, which indicates that none of the elements involved in dormancy, resistance, or germination has been removed.

A second possibility is that the exposure to PVP before freezing could alter the cation-binding properties of the cortex or extract cations from it. However, the freeze-substitution results indicated that exposure to PVP did not radically alter the cortex and, since PVP lacks chelating groups for calcium, magnesium, and manganese, one would not expect it to readily extract these ions. Furthermore, analysis of bulk samples failed to detect any significant change in the spore calcium content.

Elemental distributions. The ionic composition of spores exerts a major influence on spore formation, resistance, and dormancy. Although earlier studies (13, 23) had indicated that much of the calcium was located in the core, the composition of the cortex/coat and the distribution of other ions were not completely clear (30). The results we obtained from both the X-ray maps and the spot mode analyses now establish these elemental distributions clearly. If one assumes that the core accounts for half of the spore dry weight (probably an underestimate) and the cortex/coat layer accounts for the remainder, the results presented in Table 2 would indicate that 98% of spore calcium, 94% of spore magnesium, and 96% of spore manganese reside in the core of wild-type *B. cereus* T spores (these percentages would be even higher if the core were to account for more than half of the spore dry weight). Thus, essentially all of the divalent cations (calcium, magnesium, and manganese) are located in the core, with little or none located in the surrounding cortex/coat layers. Most of the phosphorus (presumably representing nucleic acids and energy-rich compounds such as 3-phosphoglyceric acid) is also located in the core of the spore. The phosphorus content of the cortex/coat layer probably only represents phospholipid in the membranes at the interior and exterior surfaces of the cortex. The sulfur content of the cortex/coat layer probably reflects the high sulfur content of the proteinaceous outer coat (30). The silicon content of the cortex/coat layer may result from specific incorporation or from contamination from glassware or from silicone vacuum oils employed in the apparatus used to freeze-dry the spores. Since there was considerable variation in silicon content both within and between different spore preparations, we considered it unlikely that the effect could be due entirely to contamination. The presence of the silicon might explain the ash deposits seen at the periphery of spores after microincineration (28).

Studies based on UV irradiation (8) and beta-attenuation analysis (15) have indicated that the bulk of the spore dipicolinic acid is also located in the core. Since dipicolinic acid is known to form stable and insoluble chelates with divalent cations such as calcium and since it is the major contributor to the anion population of the spore (30), it is likely that a substantial proportion of the divalent cations are bound to dipicolinic acid in the core, although this interpretation has been questioned on the basis of Raman spectroscopy (32). In this respect, our finding that virtually all the divalent cations are located in the core is consistent with the studies (8, 15) implying dipicolinic acid is located primarily in the core. However, it is important to note that substantial quantities of the divalent cations are found in the core of the mutant lacking dipicolinic acid. This indicates that not all of the divalent cations are bound to dipicolinic acid, with some probably bound to phosphate esters or aspartic and glutamic acids as suggested, for example, by Warth (30). It is also noteworthy that the magnesium and manganese concentrations in the mutant spores are somewhat lower than those in the wild-type spores. These results taken together indicate that it is likely that dipicolinic acid may bind some magnesium and manganese in addition to calcium in the wild-type spores.

It is not immediately clear why portions of calcium, manganese, magnesium, and phosphorus are clustered into granules in the mutant spores. It is possible that similar clusters might exist in the wild-type spores but that they are not so easily seen because of the substantially higher background metal ion concentration (about 950 mmol/kg as compared with less than 200 mmol/kg in the mutant spores). Alternatively, it is possible that these cations are accumulated even in the absence of dipicolinic acid but that then their free concentration is much higher, which leads to the precipitation of metal-phosphate granules. However, since it appears likely that these ions also bind to phosphate esters in the wild-type spores (30), we tend to favor the former hypothesis, although there is no reason why both explanations may not be correct. Based on the known composition of bacterial spores (30), it would seem conceivable that the phosphorus component of the granules is 3-phosphoglyceric acid. This could offer at least a partial mechanism for the ametabolic state of the dormant spores, since it is quite likely that such insoluble phosphoglycerate salts could prove to be unsatisfactory substrates for the production of energy.

Implications for theories of spore resistance and dormancy. The core location of the major divalent cations of spores tends to refute the contractile cortex theory (16) and the expanded cortex theory (9), which both demand a substantial concentration of positively charged counterions in association with the negatively

charged cortical peptidoglycan polymer. Any basic mechanism of heat resistance needs to invoke a role for the core location of these cations. The protective chelate cement theory (10) requires a high concentration of calcium chelated to dipicolinic acid in a matrix involving spore ligands, such as amino acids and peptides, to stabilize heat-labile components. This theory is not stated formally in sufficient detail to discern whether it would require all of the metal cations to be located in the protoplast, but it would certainly require a major proportion. The observed reduction in protoplast volume during sporulation, whether brought about by the proposed syneresis model (3, 20) or by some other method, appears to slightly precede the uptake of calcium ions and dipicolinic acid formation. However, the loss of granularity and the development of refractility of the forespore are clearly associated with calcium uptake, dipicolinic acid formation, and development of heat resistance. The forespore protoplast may attain a homogeneous state well before either the cortex or coats have been completely formed. Hence, development may certainly be nonsequential in the forespore. These changes are indicative of the profound alteration in the biophysical state of the forespore protoplast (7). The location of the majority of the cations in this region supports the concept of ionic involvement (3) in the controlled reordering (macromolecular rearrangement) of the nucleic acids and proteins which occurs in the spore protoplast, endowing it with resistance to heat and other agents. Further biophysical definition of this concentrated cation region is clearly required to explain the dormancy and resistance properties of the spore.

ACKNOWLEDGMENTS

We thank John Silcox, Ken McGinnis, Cindy Murray, Doug Ohye, Will Rushton, Alan Warth, and Don Fraser for their assistance and comments.

This work was supported in part by Public Health Service grants HL15835 to the Pennsylvania Muscle Institute and GM00092, both from the National Institutes of Health.

LITERATURE CITED

1. **Ando, Y.** 1976. Some properties of ionic forms of a *Clostridium perfringens* strain. Nippon Saikingaku Zasshi **31**:713-717.
2. **Aoki, H., and R. A. Slepecky.** 1974. The formation of *B. megaterium* spores having increased heat and radiation resistance and variable heat shock requirements due to manganous ions, p. 95-102. *In* A. N. Barker, G. W. Gould, and J. Wolf (ed.), Spore research 1973. Academic Press., Inc., London.
3. **Echlin, P., H. le B. Shaer, B. O. C. Gardiner, F. Franks, and M. H. Asquith.** 1977. Polymeric cryoprotectants in the preservation of biological ultrastructure. II. Physiological effects. J. Microsc. **110**:239-256.
4. **Franks, F., M. H. Asquith, C. C. Hammond, H. le B. Skaer, and P. Echlin.** 1977. Polymeric cryoprotectants in the preservation of biological ultrastructure. I. Low temperature states of aqueous solutions of hydrophilic polymers. J. Microsc. **110**:223-238.
5. **Franzini-Armstrong, C., H. E. Heuser, R. S. Reese, A. P. Somlyo, and A. V. Somlyo.** 1978. T-tubule swelling in hypertonic solutions: a freeze substitution study. J. Physiol. (London) **283**:133-140.
6. **Gerhardt, P., and S. H. Black.** 1961. Permeability of bacterial spores. II. Molecular variables affecting solute permeation. J. Bacteriol. **82**:750-760.
7. **Gerhardt, P., and W. G. Murrell.** 1978. Basis and mechanism of spore resistance: a brief preview, p. 18-20. *In* G. Chambliss and J. C. Vary (ed.), Spores VII. American Society for Microbiology, Washington, D.C.
8. **Germaine, G. R., and W. G. Murrell.** 1974. Use of ultraviolet radiation to locate dipicolinic acid in *Bacillus cereus* spores. J. Bacteriol. **118**:202-208.
9. **Gould, G. W., and G. J. Dring.** 1975. Heat resistance of bacterial endospores and the concept of an osmoregulatory cortex. Nature (London) **258**:402-405.
10. **Grecz, N., R. F. Smith, and C. C. Hoffmann.** 1970. Sorption of water by spores, heat killed spores and vegetative cells. Can. J. Microbiol. **16**:573-579.
11. **Hall, T. A.** 1971. The probe X-ray microassay of chemical elements, p. 157-275. *In* G. Oster (ed.), Physical techniques in biological research, vol. 1A, 2nd ed. Academic Press, Inc., New York.
12. **Keynan, A., W. G. Murrell, and H. O. Halvorson.** 1962. Germination properties of spores with low dipicolinic acid content. J. Bacteriol. **83**:395-399.
13. **Knaysi, G.** 1965. Further observations on the spodograms of *Bacillus cereus* endospores. J. Bacteriol. **90**:453-455.
14. **Kovacs-Proszt, G., and J. Farkas.** 1976. Resistance of *B. cereus* spores as affected by changes in their exchangeable Ca content. Acta Aliment. Acad. Sci. Hung. **5**:179-188.
15. **Leanz, G. F., and C. Gilvarg.** 1974. Localization of bacterial spore components by beta attenuation analysis, p. 45-48. *In* H. O. Halvorson, R. Hanson, and L. L. Campbell (ed.), Spores V. American Society for Microbiology, Washington, D.C.
16. **Lewis, J. C., N. S. Snell, and H. K. Burr.** 1960. Water permeability of bacterial spores and the concept of a contractile cortex. Science **132**:544-545.
17. **Marshall, B. J., and W. G. Murrell.** 1970. Biophysical analysis of the spore. J. Appl. Bacteriol. **33**:103-129.
18. **Murrell, W. G.** 1967. The biochemistry of the bacterial endospore. Adv. Microbiol. Physiol. **1**:133-251.
19. **Murrell, W. G.** 1969. Chemical composition of spores and spore structures, p. 215-273. *In* G. W. Gould and A. Hurst (ed.), The bacterial spore. Academic Press., Inc., New York.
20. **Murrell, W. G.** 1978. Development of the heat resistant state in bacterial spores. Spore Newsl. **6**(special issue): 27-28.
21. **Murrell, W. G., D. F. Ohye, and R. A. Gordon.** 1969. Cytological and chemical structure of the spore, p. 1-19. *In* L. L. Campbell (ed.), Spores IV. American Society for Microbiology, Bethesda, Md.
22. **Murrell, W. G., and A. D. Warth.** 1965. Composition and heat resistance of bacterial spores. p. 1-24. *In* L. L. Campbell and H. O. Halvorson (ed.), Spores III. American Society for Microbiology, Bethesda, Md.
23. **Scherrer, R., and P. Gerhardt.** 1972. Location of calcium within *Bacillus* spores by electron probe X-ray microanalysis. J. Bacteriol. **112**:559-568.
24. **Shuman, H., A. P. Somlyo, and A. V. Somlyo.** 1976. Quantitative electron probe microanalysis of biological thin sections. Ultramicroscopy **1**:317-339.
25. **Somlyo, A. V., H. Shuman, and A. P. Somlyo.** 1977. The composition of the sarcoplasmic reticulum in situ: electron probe X-ray microanalysis of cryosections. J. Cell Biol. **74**:828-857.
26. **Somlyo, A. P., A. V. Somlyo, and H. Shuman.** 1979.

Electron probe analysis of vascular smooth muscle. J. Cell Biol. **81**:316–335.

27. **Somlyo, A. P., A. V. Somlyo, H. Shuman, and M. Stewart.** 1979. Electron probe analysis of muscle and X-ray mapping of biological specimens with a field emission gun. Scanning Electron Microsc. **2**:711–722.
28. **Thomas, R. S.** 1964. Ultrastructural localization of mineral matter in bacterial spores by microincineration. J. Cell Biol. **23**:113–133.
29. **Thomas, R. S., M. M. Millard and R. Scherrer.** 1976. Electron microscopy and X-ray photoelectron spectroscopy of oxygen plasma-etched bacterial spores and cells p. 134–135. *In* Proceedings of the 34th EMSA Meeting. Claitor's Publishing Division, Baton Rouge, La.
30. **Warth, A. D.** 1979. Molecular structure of the bacterial spore. Adv. Microbiol. Physiol. **17**:1–45.
31. **Warth, A. D.** 1979. Estimation of dipicolinic acid in bacterial spores and foods by liquid chromatography. Appl. Environ. Microbiol. **38**:1029–1033.
32. **Woodruff, W. H., T. G. Spiro, and C. Glivag.** 1974. Raman spectroscopy *in vivo*: evidence on the structure of dipicolinate in intact spores of *B. megaterium*. Biochem. Biophys. Res. Commun. **58**:197–203.
33. **Young, E., and P. C. Fitz-James.** 1962. Chemical and morphological studies of bacterial spore formation. J. Cell Biol. **12**:115–133.